Published in final edited form as:
J Neural Eng. 2018 August ; 15(4): 046002. doi:10.1088/1741-2552/aab790.

Sensory adaptation to electrical stimulation of the somatosensory nerves

Emily L. Graczyk[1,2,†], **Benoit P. Delhaye**[3,†], **Matthew A. Schiefer**[1,2], **Sliman J. Bensmaia**[3], and **Dustin J. Tyler**[1,2,*]

[1]Department of Biomedical Engineering, Case Western Reserve University, Cleveland, OH 44106

[2]Cleveland Louis-Stokes Department of Veteran's Affairs Medical Center, Cleveland, OH 44106

[3]Department of Organismal Biology and Anatomy, University of Chicago, Chicago, IL 60637

Abstract

Sensory systems adapt their sensitivity to ambient stimulation levels to improve their responsiveness to changes in stimulation. The sense of touch is also subject to adaptation, as evidenced by the desensitization produced by prolonged vibratory stimulation of the skin. Electrical stimulation of residual nerves elicits tactile sensations that can convey feedback for bionic limbs. In this study, we investigate whether this artificial touch is also subject to adaptation, despite the fact that the sites of mechanotransduction are bypassed. We characterize the time course and magnitude of the sensory adaptation caused by extended electrical stimulation of the residual somatosensory nerves in three patients implanted with cuff electrodes. We find that the time course and magnitude of electrically induced adaptation are very similar to their mechanically induced counterparts. We conclude that, in natural touch, the process of mechanotransduction is not required for adaptation and artificial touch naturally experiences adaptation-induced adjustments of the dynamic range of sensations.

Introduction

Adaptation – the progressive desensitization to prolonged, suprathreshold stimulation – is a ubiquitous phenomenon in the nervous system, one that has been extensively documented in all sensory systems. For example, vision is far more sensitive in the dark than it is in daylight (Hecht, 1920). The function of adaptation is to adjust sensitivity to reduce responsiveness to ambient stimulation levels and to promote responsiveness to changes in stimulation (Brenner et al., 2000). Visual adaptation is a key reason why we can see across eight orders of magnitude of ambient illumination.

The sense of touch is also subject to adaptation, as evidenced by the progressive perceptual and neuronal desensitization caused by prolonged vibrotactile stimulation of the skin. In psychophysical experiments, suprathreshold vibrotactile stimulation results in an increase in

*Corresponding author: Dustin J. Tyler, PhD, Department of Biomedical Engineering, Case Western Reserve University, 10900 Euclid Ave, Cleveland, OH 44106, dustin.tyler@case.edu.
†These authors contributed equally to this work.

Conflict of Interest: The authors declare no competing financial interests.

detection threshold and a progressive decrease in the subjective magnitude of the stimulus (Hahn, 1966; Gescheider and Wright, 1968; Berglund and Berglund, 1970; Verrillo and Gescheider, 1977; Hollins et al., 1990). The degree of adaptation increases as the amplitude of the conditioning stimulus increases and also depends on its frequency (Verrillo and Gescheider, 1977; Hollins et al., 1990). The frequency-dependence of adaptation reflects, in part, the frequency-sensitivity profiles of the different classes of tactile nerve fibers: fibers that are more sensitive to a stimulus will tend to be more desensitized by it. Higher frequencies also tend to adapt nerve fibers more strongly (Hollins et al., 1990; Bensmaïa et al., 2005).

Vibrotactile adaptation is caused in part by changes in skin elasticity that impact the transmission of vibrations through the skin (Hahn, 1966). However, a major contributor to vibrotactile adaptation is a desensitization of the nerve fibers themselves, caused by a progressive increase in their spike-generation threshold (Ribot-Ciscar et al., 1996; Bensmaïa et al., 2005). Finally, central desensitization also plays a role in the observed perceptual adaptation as evidenced by the fact that the latter operates on a slower time scale than does its neuronal counterpart at the periphery (Leung, Bensmaïa, Hsiao, & Johnson, 2005).

While adaptation has been extensively documented for natural tactile stimulation, less is known about whether direct activation of neurons through electrical stimulation also leads to adaptation. Indeed, sensory adaptation has been shown to occur with electrocutaneous stimulation (Szeto and Saunders, 1982; Kaczmarek et al., 1991; Kaczmarek, 2000; Buma et al., 2007), but this effect may be, at least in part, mediated by a desensitization of the mechanotransduction sites. Characterizing adaptation when mechanoreceptors are bypassed is important for understanding the mechanism of adaptation and for the development of bionic limbs for amputees that provide artificial tactile feedback by electrically stimulating the nerve through chronically implanted neural interfaces. Patterned electrical stimulation of the nerve has been shown to evoke tactile percepts and improve the performance of hand prosthesis users on functional tasks (Clark et al., 2014; Raspopovic et al., 2014; Tan et al., 2014; Graczyk et al., 2016; Oddo et al., 2016; Schiefer et al., 2016). Having previously observed that extraneural stimulation of the nerve seems to cause adaptation (Graczyk et al., 2016), we sought in the present study to assess its magnitude, its dependence on stimulation parameters, and its time course using well-established psychophysical experimental paradigms. We then compare the effects of adaptation on artificial touch to those observed with natural tactile stimulation and discuss the implications of our results on the design of sensory encoding algorithms for bionic hands.

Methods

Subjects

Three male human volunteers with unilateral, upper limb loss (two right arm and one left arm) participated in this study. Subject 1 has a right trans-radial amputation due to a traumatic injury in 2010 and was implanted with two 8-contact flat interface nerve electrodes (FINEs) around his median and ulnar nerves and a 4-contact CWRU spiral electrode around his radial nerve in 2012. Subject 2 has a right trans-radial amputation due to a traumatic injury in 2004 and was implanted with three 8-contact FINEs around his

median, ulnar, and radial nerves in 2013. Subject 3 has a left trans-radial amputation due to a traumatic injury in 2013 and was implanted with two 16-contact FINEs around his median and ulnar nerves in 2016. The subjects came to the laboratory for 6 hour testing sessions every 2–6 weeks, depending on their availability. The present study took place in months 47 to 62 post-implantation for subject 1, months 38 to 54 post-implantation for subject 2, and month 15 post-implantation for subject 3. All study devices and procedures were reviewed and governed by the U.S. Food and Drug Administration Investigational Device Exemption, the Cleveland Department of Veterans Affairs Medical Center Institutional Review Board, and the Department of the Navy Human Research Protection Program. Informed consent was obtained from all subjects.

Electrical stimuli

Trains of square, bi-phasic, current-controlled, cathode-first stimulation pulses were delivered to individual contacts within the electrodes.

Detection thresholds

Before starting the experiment, a rough estimate of the subject's detection threshold was obtained. Pulse frequency (PF) was set to 100 Hz, pulse width (PW) to 255 microseconds, and pulse amplitude (PA) to 0.3 mA, and each stimulation train lasted for 5 seconds. Because the PA resolution of our stimulator was fairly coarse and we aimed to operate stimulation on the right side of the strength-duration curve, we first increased PA until sensation was reported, then decreased PW to find the detection threshold. PA was increased in steps of 0.1 mA in successive trials until sensation was reported. A two-alternative forced-choice tracking paradigm was used to find the minimum detectable PW at this PA: Starting at 130 microseconds, PW was decremented by $130/2^n$ when the subject reported sensation or incremented by this same amount when the subject did not (where n is the number of reversals). To allow a sufficient range of PWs above threshold for the conditioning stimulus (described below), if the minimum detectable PW was greater than 150 microseconds, the PA was increased again by 0.1 mA and the tracking paradigm was repeated to find the minimum detectable PW at this new PA. This process was repeated until the minimum detectable PW was below 150 microseconds. This threshold estimation served as an initial starting point for the experiments described below. In addition, PWs in the experimental range were briefly tested to ensure that all sensations were comfortable.

A single experimental block consisted of first finding the unadapted detection threshold, then administering a suprathreshold conditioning stimulus for 2 minutes, then finding the adapted threshold (Figure 1A). Thresholds in the experimental block were measured by the method of constant stimuli (Gescheider, 2013), with each threshold measurement consisting of 70 trials. On each trial, two sequential stimulus intervals were indicated by a visual display, each lasting 1 s with a 1-s inter-stimulus interval. One of the intervals contained a stimulus and the subject's task was to indicate which one by pressing one of two keys. A 4-s inter-trial interval was enforced, which included the response time. Seven PWs spaced over a broad range were each tested 10 times in pseudo-random order. Whether the stimulus was presented in the first or second interval was randomized. The same set of PWs was tested for both the unadapted and adapted thresholds. On adapted trials, the conditioning stimulus was

presented during the first three seconds of the 4-s inter-trial interval to maintain the level of adaptation. Each experimental block lasted approximately 30 minutes.

This procedure was repeated for twelve electrode contacts in two subjects (subjects 1 and 2) and in six different experimental sessions (two contacts per session). Four to six experimental blocks were administered per session, with the electrode contacts interleaved to allow for recovery from adaptation between successive blocks. To determine the effect of the conditioning stimulus intensity on threshold shift, one parameter of the conditioning stimulus (either PW or PF) was systematically varied across three different levels within a single experimental session, while the other conditioning stimulus parameters were held constant. When PW was varied (eight contacts), the PF was fixed at 100 Hz and the conditioning stimuli took on one of three values of PW: low (~10–50 μs above detection threshold), mid (~50–100 μs above detection threshold), or high (~100–150 μs above detection threshold). When PF was varied (four contacts), the PW was fixed at a suprathreshold value and the PF of the conditioning stimulus was 25, 50, or 200 Hz.

The proportion of correct detections as a function of PW was described by a normal cumulative density function, fit using Bayesian inference methods (psignifit 3.0 Matlab toolbox, see Fründ, Haenel, & Wichmann, 2011). The detection threshold is the PW corresponding to 75% correct performance. The adaptation effect for each block is the magnitude of the threshold elevation caused by the conditioning stimulus. For the purposes of inference testing, we computed the z-score of the adaptation effects obtained from each lead to pool data across leads.

Intensity tracking

First, a rough estimate of the detection threshold was found as described above and a comfortable range of supra-threshold test PWs was chosen. Then, the test (supra-threshold) stimulus was presented to the subject with constant PW, PA, and PF for 3 minutes without interruption (Figure 1B). Every ten seconds, an auditory cue signaled the subject to indicate the perceived magnitude of the sensation on a visual-analog scale presented on a computer screen. Each stimulus was presented three times. In a single experimental session, four electrode contacts were tested in interleaved order, to allow for recovery from adaptation between successive tests of the same lead. The contacts tested within a session were selected to be as far apart in the cuff as possible and such that the projected fields did not overlap to minimize the likelihood that overlapping fiber populations were activated in consecutive test blocks. To test the effect of PW and PF on adaptation, several different supra-threshold PWs (2 to 4 suprathreshold PWs) or PFs (25, 50, 100 and/or 200Hz) were presented on separate trials within a single experimental session. A total of 24 contacts were tested in 14 sessions across three subjects, yielding a total of 295 trials.

Perceived intensity, tracked every ten seconds during 3 minutes, was expressed as a percentage of initial perceived intensity. The percent intensity as a function of time was fit with a piecewise function, using *lsqcurvefit* in Matlab. In the first part of the function, the intensity is a constant set to 100% for a variable duration, typically lasting around 10 seconds, as this is the period characterized by no discernible adaptation. In the second part, the intensity follows an exponential decay, captured by the following function:

$$I(t) = \begin{cases} 100\,\%, & t < d \\ A * \mathrm{e}^{\left(\frac{-t-d}{\tau}\right)} + (100 - A), & t \geq d \end{cases}$$

where A is the magnitude of the intensity decay (in %), τ is the time constant (in seconds) and d is a delay that captures the duration of the first part (in seconds). A, τ, and d are free parameters. Time constant estimates are highly sensitive to noisy data. With this in mind, we discarded trials in which traces were poorly fit by an exponential ($R^2 < 0.7$). We also discarded trials where decay was extreme (A<10% or A>95%) because these also yielded poor estimates of the time constants. Time constants were transformed logarithmically for the purposes of inference testing because they were log-normally distributed.

Experimental Design and Statistical Analysis

For the detection threshold experiments, adapted thresholds were compared to unadapted thresholds using paired t-tests. Pearson's correlation coefficients were used to determine the impact of conditioning stimulation levels on threshold elevation. For the intensity tracking experiments, perceived intensity at the end of the trials was compared to initial intensity using a one-sample t-test. Pearson's correlation coefficients were used to determine the impact of stimulation PW and PF on decay rate and decay amplitude. Within-trial comparisons between stimulation levels were performed using paired t-tests. All statistical tests were performed in MATLAB with alpha level set to 0.05.

Results

Detection thresholds

First, we examined the degree to which perceptual sensitivity to electrical stimulation of the nerve is affected by extended supra-threshold electrical stimulation. Sensitivity was quantified by the detection threshold using a standard two-alternative forced choice paradigm (Figure 1A). Threshold estimates obtained before the application of a conditioning stimulus were consistent across blocks (Figure 2, black traces). This confirms that the approach provided reliable threshold estimates and that thresholds recover to baseline following periods of no stimulation. The same threshold paradigm was then repeated after administering a conditioning stimulus for 2 minutes. In all cases, the conditioning stimulus reduced perceptual sensitivity to electrical stimulation, as shown by a systematic rightward shift in the psychometric functions and an increase in detection thresholds (see Figure 2, red traces, and Figure 3A). The adapted threshold was significantly greater than the corresponding unadapted threshold in 33 of 36 experimental blocks, and this effect was highly significant (pooled data across sessions and subjects, paired t-test, $t(35)=10.21$, $p \ll 0.001$). The magnitude of the threshold elevation increased as the PW or PF of the conditioning stimulus increased as evidenced by a significant correlation between the PW or PF of the conditioning stimulus and threshold shift ($r=0.76$, $p \ll 0.001$, $n=25$, for the PW manipulations, see Figure 3B; $r=0.89$, $p<0.001$, $n=11$, for the PF manipulations, see Figure 3C).

Intensity tracking

Next, we examined the time course of adaptation. Subjects rated the perceived intensity of a constant stimulus every ten seconds for the duration of the stimulus, which lasted 180 s (Figure 1B). The perceived intensity decreased significantly over the duration of the stimulus (Figure 4, mean decay = 65.01%, $t(203)=41.39$, $p \ll 0.001$). Indeed, after a short delay (median of 11 seconds), intensity decayed approximately exponentially with a median time constant of 30 seconds (Figure 5A). Fitted time constants were consistent across contacts within subject, but varied across subjects (Figure 5A). From examination of the aggregate data, time constants seemed to be only weakly dependent on stimulus intensity: τ increased slightly with increases in PW ($r=0.20$, $p=0.007$, $n=174$, Figure 5B) but was nearly independent of PF ($r=-0.04$, $p=0.53$, n=204, Figure 5C). However, on sessions that included trials at different stimulation intensity levels (varying either PW or PF, with all other parameters kept constant), no trends were observed (paired t-test, $t(9)=-0.81$, $p=0.44$ for PW; $t(20)=0.16$, $p=0.88$ for PF, 25Hz compared to 200Hz, see lines in Figure 5B–C), suggesting that the effect observed in the aggregate data is artefactual. Furthermore, there was no correlation between stimulation parameters and the degree of decay ($r=0.04$, $p=0.61267$, $n=174$, for PW and $r=-0.13$, $p=0.06579$, $n=204$, for PF).

Discussion

Comparison with natural vibrotactile adaptation

Time course of adaptation—When the skin is subjected to prolonged vibrotactile stimulation, tactile fibers become desensitized over an exponential time course with a time constant of about 10 s (Leung et al., 2005). In contrast, the decay time constant for vibrotactile perception is slower, ranging from 60 to 200 s based on threshold measurements (Hahn, 1966, 1968, Hollins et al., 1990, 1991) and 20 to 400 s based on measurements of perceived intensity (Hahn, 1966; Berglund and Berglund, 1970). The time course of electrically induced sensory adaptation reported here, ranging from 10 to 100 seconds, thus spans the same range as its vibrotactile counterpart. Comparable time constants, spanning 30 to 200 seconds, have been observed for electrocutaneous adaptation (Buma et al., 2007). Furthermore, the observed across-subjects variability in time course has also been reported in the vibrotactile literature (Berglund and Berglund, 1970). Therefore, electrically induced adaptation operates over a similar time course as its mechanically induced counterpart.

Effect of adapting amplitude—For vibrotactile stimulation, threshold shift is a power function of conditioning stimulus intensity relative to threshold, with an exponent ranging from 0.5 to 0.7 (Hahn, 1966; Verrillo and Gescheider, 1977; Hollins et al., 1990). Similarly, we observed a power function relating threshold and conditioning stimulus intensity (PW), as evidenced by a linear relationship plotted in log-log coordinates, with a slope of 0.55 (see also Figure 5B). Increasing the amplitude of a vibratory stimulus applied to the skin and increasing the width of electrical pulses in a stimulation train both result primarily in the recruitment of additional nerve fibers (Johnson, 1974; Muniak et al., 2007), which explains why these two manipulations have similar adaptation effects.

Effect of adapting frequency—For vibrotactile stimulation, the dependence of adaptation effects on frequency can be explained in terms of the frequency sensitivity of the different afferent populations, determined primarily by their mechanoreceptors (Cauna et al., 1966; Loewenstein and Skalak, 1966; Iggo and Ogawa, 1977). The extent to which a conditioning stimulus activates a given population of afferents determines the extent to which these will become adapted (Gescheider and Wright, 1968; Verrillo and Gescheider, 1977; Hollins et al., 1990). For example, high-frequency stimulation (~250 Hz) selectively desensitizes PC fibers whereas low-frequency stimulation (~10 Hz) primarily desensitizes SA1 and RA fibers. However, higher vibrotactile frequencies also tend to result in greater adaptation effects on individual nerve fibers, over the range of frequencies to which the fiber is sensitive (Bensmaïa et al., 2005). In contrast, increasing the frequency of an electrical pulse train leads to an increase in the firing rate of all stimulated fibers, regardless of submodality. As a result, increased PF leads to increased thresholds across the entire range of frequencies. Differences in the effect of frequency on electrically and mechanically induced adaptation can thus be explained by the different ways in which frequency impacts the evoked neural response in the two modalities.

Implications for the mechanism of adaptation

The parsimonious explanation for the remarkable similarity in the time courses and action spectra of mechanically and electrically induced adaptation is that they are mediated by the same neural mechanisms. Given that electrical stimulation of the nerve bypasses the mechanoreceptors, we can conclude that the process of mechanotransduction is not necessary for perceptual adaptation to occur. Thus, both electrically-induced and mechanically-induced adaptation are not governed solely by the process of mechanotransduction, but rather by a downstream mechanism, for example an increase in spike generation threshold or synaptic mechanisms in the central nervous system, consistent with previous conjecture (O'Mara et al., 1988; Bensmaïa et al., 2005).

Implications for neuroprosthetics

During sustained grasp with a bionic hand, the nerve may be electrically stimulated for extended periods of time. The resulting progressive desensitization to stimulation may be interpreted as a result of stimulation-induced injury of neural fibers. However, as with its mechanically-induced counterpart, electrically-induced adaptation is reversible and sensitivity returns to its unadapted state minutes after stimulation ceases, as demonstrated by the close similarity in unadapted detection thresholds across successive blocks of threshold measurements (see Fig. 2). Furthermore, one might decide to compensate for the resulting desensitization by progressively increasing the gain of the stimulator in a stimulation-dependent manner. However, adaptation to natural stimulation is adaptive in the sense that it diminishes the response to constant and therefore uninformative stimulation and renders the nervous system more responsive to *changes* in stimulation, which are more informative (Brenner et al., 2000). The remarkable similarities between electrically-induced adaptation and its mechanical counterpart suggest that no compensation in electrical stimulation is necessary: The dynamic range of the nerve response will shift according to mean level of stimulation in the same way with electrical stimulation as it would with mechanical stimulation, thereby maximizing the usefulness and naturalness of this artificial

somatosensory input. Electrically induced adaptation thus invokes similar neural mechanisms as natural adaptation and closely mimics the function of natural adaptation, enabling more responsive and functional sensory prostheses.

Acknowledgments

We would like to thank I. Cuberovic and M. Schmitt for assistance with subject scheduling and data collection. This work was sponsored by the DARPA Biological Technologies Office (BTO) HAPTIX program under the auspices of Dr. D. Weber through the Space and Naval Warfare Systems Center (Pacific contract no. NC66001-15-C-4041), by the U.S. Department of Veterans Affairs Rehabilitation Research and Development Service Program (Merit Review Award #I01 RX00133401 and Center #C3819C), and by the NSF (grant no. DGE-1451075). The content is solely the responsibility of the authors and does not necessarily represent the official views of the listed funding institutions. All data is available through data transfer agreement upon request to D.J.T.

References

Bensmaïa SJ, Leung YY, Hsiao SS, Johnson KO. Vibratory adaptation of cutaneous mechanoreceptive afferents. J Neurophysiol. 2005; 94:3023–3036. Available at: http://www.ncbi.nlm.nih.gov/pubmed/16014802%5Cnhttp://www.pubmedcentral.nih.gov/articlerender.fcgi?artid=PMC1994926. [PubMed: 16014802]

Berglund U, Berglund B. Adaptation and recovery in vibrotactile perception. Percept Mot Skills. 1970; 30:843–853. [PubMed: 5429335]

Brenner N, Bialek W, de Ruyter van Steveninck R. Adaptive rescaling maximizes information transmission. Neuron. 2000; 26:695–702. [PubMed: 10896164]

Buma DG, Buitenweg JR, Veltink PH. Intermittent stimulation delays adaptation to electrocutaneous sensory feedback. IEEE Trans Neural Syst Rehabil Eng. 2007; 15:435–441. [PubMed: 17894276]

Cauna N, de Reuck AV, Knight J. Fine structure of the receptor organs and its probable functional significance. Touch, Heat Pain. 1966:117–127.

Clark, GA., Wendelken, S., Page, DM., Davis, T., Wark, HAC., Normann, RA., Warren, DJ., Hutchinson, DT. Using multiple high-count electrode arrays in human median and ulnar nerves to restore sensorimotor function after previous transradial amputation of the hand. 2014 36th Annual International Conference of the IEEE Engineering in Medicine and Biology Society, EMBC 2014; 2014. p. 1977-1980.

Fründ I, Haenel NV, Wichmann FA. Inference for psychometric functions in the presence of nonstationary behavior. J Vis. 2011; 11:16.

Gescheider, GA. Psychophysics: The Fundamentals. 3. Mahway, New Jersey: Lawrence Erlbaum Associates, Inc; 2013.

Gescheider, Ga, Wright, JH. Effects of sensory adaptation on the form of the psychophysical magnitude function for cutaneous vibration. J Exp Psychol. 1968; 77:308–313. [PubMed: 5655125]

Graczyk EL, Schiefer MA, Saal HP, Delaye BP, Bensmaia SJ, Tyler DJ. The neural basis of perceived intensity in natural and artificial touch (accepted). Sci Transl Med. 2016; 142:1–11.

Hahn JF. Vibrotactile adaptation and recovery measured by two methods. J Exp Psychol. 1966; 71:655–658. [PubMed: 5939703]

Hahn JF. Low-frequency vibrotactile adaptation. J Exp Psychol. 1968; 78:655–659. [PubMed: 5705870]

Hecht S. The dark adaptation of the human eye. J Gen Physiol. 1920; 2:499–517. [PubMed: 19871826]

Hollins M, Delemos Ka, Goble aK. Vibrotactile adaptation on the face. Percept Psychophys. 1991; 49:21–30. [PubMed: 2011449]

Hollins M, Goblea K, Whitsel BL, Tommerdahl M. Time course and action spectrum of vibrotactile adaptation. Somatosens Mot Res. 1990; 7:205–221. [PubMed: 2378193]

Iggo A, Ogawa H. Correlative physiological and morphological studies of rapidly adapting mechanoreceptors in cat's glabrous skin. J Physiol. 1977; 266:275–296. [PubMed: 853451]

Johnson KO. Reconstruction of population response to a vibratory stimulus in quickly adapting mechanoreceptive afferent fiber population innervating glabrous skin of the monkey. J Neurophysiol. 1974; 37:48–72. [PubMed: 4204567]

Kaczmarek KA. Electrotactile Adaptation on the Abdomen Copy: Preliminary Results. IEEE Trans Rehabil Eng. 2000; 8:499–505. [PubMed: 11204041]

Kaczmarek, Ka, Webster, JG., Bach-y-Rita, P., Tompkins, WJ. Electrotactile and vibrotactile displays for sensory substitution systems. IEEE Trans Biomed Eng. 1991; 38:1–16. Available at: http://www.ncbi.nlm.nih.gov/pubmed/2026426. [PubMed: 2026426]

Leung YY, Bensmaia SJ, Hsiao SS, Johnson KO. Time-course of vibratory adaptation and recovery in cutaneous mechanoreceptive afferents. J Neurophysiol. 2005; 94:3037–3045. Available at: http://www.ncbi.nlm.nih.gov/pubmed/16014802%5Cnhttp://www.pubmedcentral.nih.gov/articlerender.fcgi?artid=PMC1994926. [PubMed: 16222071]

Loewenstein WR, Skalak R. Mechanical transmission in a Pacinian corpuscle. An analysis and a theory. J Physiol. 1966; 182:346–378. [PubMed: 5942033]

Muniak, Ma, Ray, S., Hsiao, SS., Dammann, JF., Bensmaia, SJ. The neural coding of stimulus intensity: linking the population response of mechanoreceptive afferents with psychophysical behavior. J Neurosci. 2007; 27:11687–11699. [Accessed September 16, 2013] Available at: http://www.ncbi.nlm.nih.gov/pubmed/17959811. [PubMed: 17959811]

O'Mara S, Rowe MJ, Tarvin RP. Neural mechanisms in vibrotactile adaptation. J Neurophysiol. 1988; 59:607–622. [PubMed: 3351576]

Oddo CM, Raspopovic S, Artoni F, Mazzoni A, Spigler G, Petrini F, Giambattistelli F, Vecchio F, Miraglia F, Zollo L, Di Pino G, Camboni D, Carrozza MC, Guglielmelli E, Rossini PM, Faraguna U, Micera S. Intraneural stimulation elicits discrimination of textural features by artificial fingertip in intact and amputee humans. Elife. 2016; 5:1–27.

Raspopovic S, et al. Restoring natural sensory feedback in real-time bidirectional hand prostheses. Sci Transl Med. 2014; 6:222ra19. [Accessed February 20, 2014] Available at: http://www.ncbi.nlm.nih.gov/pubmed/24500407.

Ribot-Ciscar E, Roll JP, Tardy-Gervet MF, Harlay F. Alteration of human cutaneous afferent discharges as the result of long-lasting vibration. J Appl Physiol. 1996; 80:1708–1715. Available at: http://www.ncbi.nlm.nih.gov/pubmed/8727558. [PubMed: 8727558]

Schiefer M, Tan D, Sidek SM, Tyler DJ. Sensory feedback by peripheral nerve stimulation improves task performance in individuals with upper limb loss using a myoelectric prosthesis. J Neural Eng. 2016; 13:16001. Available at: http://www.ncbi.nlm.nih.gov/pubmed/26643802.

Szeto AYJ, Saunders FA. Electrocutaneous Stimulation for Sensory Communication in Rehabilitation Engineering. IEEE Trans Biomed Eng. 1982; BME-29:300–308.

Tan DW, Schiefer Ma, Keith MW, Anderson JR, Tyler J, Tyler DJ. A neural interface provides long-term stable natural touch perception. Sci Transl Med. 2014; 6:257ra138–257ra138. [Accessed October 8, 2014] Available at: http://stm.sciencemag.org/cgi/doi/10.1126/scitranslmed.3008669.

Verrillo RT, Gescheider GA. Effect of prior stimulation on vibrotactile thresholds. Sens Processes. 1977; 1:292–300. [PubMed: 918678]

Whitsel BL, Kelly EF, Quibrera M, Tommerdahl M, Li Y, Favorov OV, Xu M, Metz CB. Time-dependence of SI RA neuron response to cutaneous flutter stimulation. Somatosens Mot Res. 2003; 20:45–69. [PubMed: 12745444]

SIGNIFICANCE STATEMENT

Adaptation is an essential property of all sensory systems, endowing them with high sensitivity to *changes* in stimulation across wide ranges of ambient stimulation levels. Here, for the first time, we investigate the process of sensory adaptation through direct activation of tactile afferents in the absence of peripheral mechanotransducers. Using two psychophysical paradigms, we show that prolonged electrical stimulation of the peripheral nerves in amputees results in adaptation that is equivalent in magnitude and time course to adaptation in the intact tactile system. We conclude that processes downstream from mechanotransduction must drive adaptation. Further, as it does for native hands, adaptation confers to bionic hands enhanced sensitivity to changes in sensory stimulation and thus a more natural sensory experience.

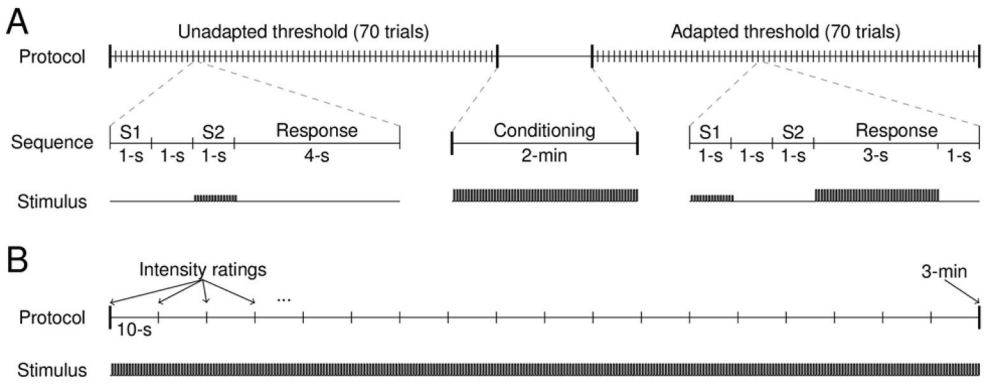

Figure 1.

Experimental protocols. A| The detection threshold experiment: the detection threshold was measured before and after a 2 minute conditioning stimulus. In each trial sequence, two 1-s stimulus intervals were presented with a 1-s intervening period. Only one interval contained a stimulus and the location of the stimulus in interval 1 or 2 was randomized. The response interval was 4 s long and contained a 3-s “boost” of the conditioning stimulus in the adapted threshold trials, but not in the unadapted threshold trials. B| The intensity tracking experiment: the intensity of a constant stimulus was rated every ten seconds for 3 minutes.

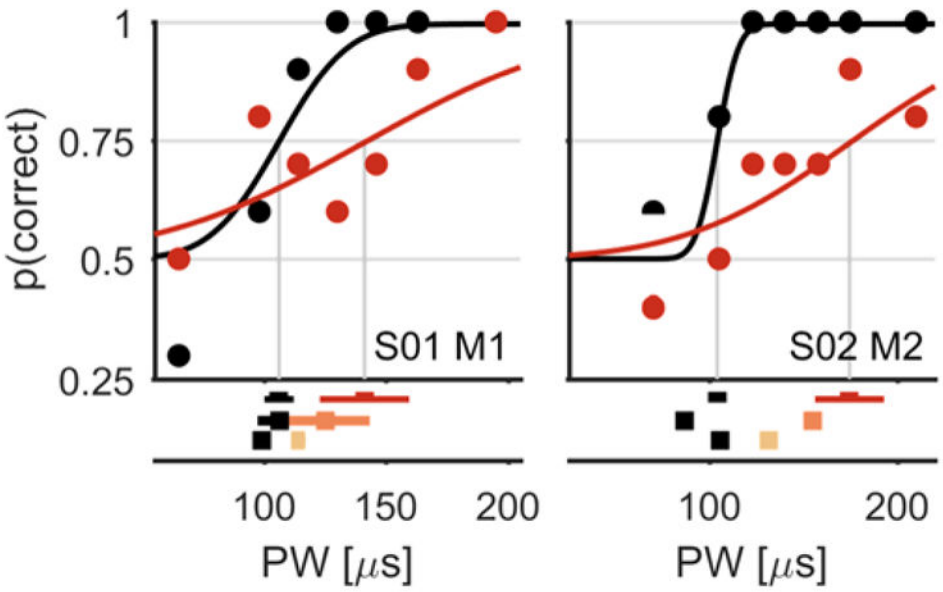

Figure 2.

Detection thresholds: top, two typical psychometric functions showing the subject's detection performance as a function of PW (for two different subjects and contacts, indicated at the bottom right of each plot). Black traces indicate unadapted threshold measurements and colored traces indicate adapted threshold measurements. Red traces show the shifted psychometric function for the highest conditioning stimulus intensity. Bottom, the subjects' detection thresholds for three different conditioning intensities (light to dark for low to high conditioning stimulus intensities, respectively). Error bars show 95% confidence intervals.

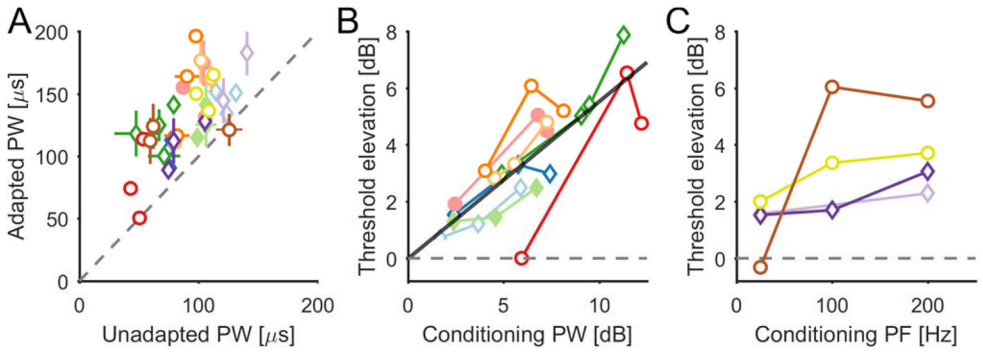

Figure 3.

Conditioning stimuli caused an increase in subjects' detection thresholds. A| Adapted detection threshold as a function of unadapted threshold. Horizontal and vertical bars indicate 95% confidence intervals. B| Detection threshold elevation as a function of conditioning PW above unadapted threshold (in dB). C| Detection threshold elevation as a function of conditioning PF (in Hz). Colors indicate different contacts and correspond across A, B and C; symbols indicate different subjects (circle for S01 and diamond for S02) and filled symbols correspond to examples shown in figure 1.

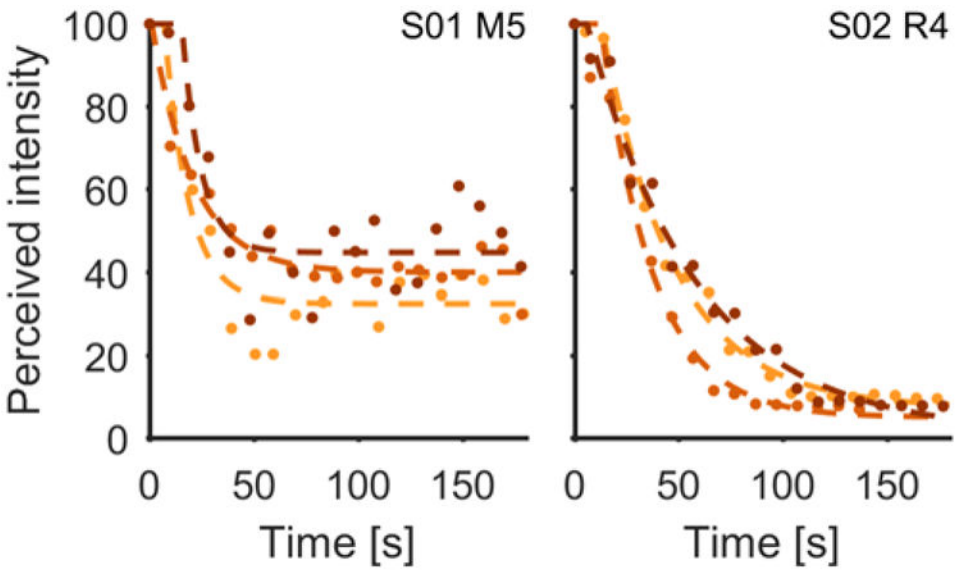

Figure 4.

Intensity tracking: two typical experimental data sets for two different subjects (S01 and S02, indicated in upper right of each plot). Perceived intensity with respect to initial perceived intensity as a function of time for three successive trials. Colors indicate the sequence of trials (bright first, dark last). Dots are raw data, dashed lines show exponential fits.

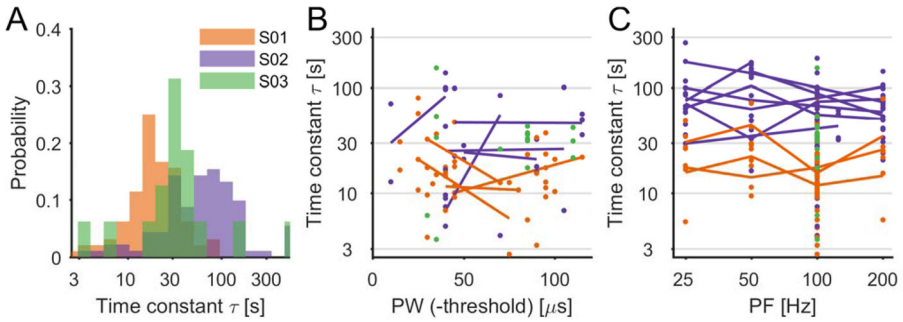

Figure 5.

Intensity decay time constants. A| Histogram for the time constant parameter for the three subjects, all trials pooled. B| Time constants plotted as a function of stimulus PW (above threshold). For these trials, PF=100Hz. C| Time constants plotted as a function of stimulus PF. For B (and C), each dot is a single trial and lines are added when multiple PW (in B) or PF (in C) were tested on the same contact and in the same session (with all other parameters constant). The lines show the average across repetitions for a given PW (or PF). In all three subpanels, colors correspond to different subjects and the time constants are shown on a logarithmic scale.